J Exp Biol Advance Online Articles. First posted online on 25 April 2013 as doi:10.1242/jeb.083352
Access the most recent version at http://jeb.biologists.org/lookup/doi/10.1242/jeb.083352

# The hydrodynamics of contact of a marine larva, *Bugula neritina*, with a cylinder

Gregory Zilman[1], Julia Novak[1], Alex Liberzon[1], Shimrit Perkol-Finkel[1], Yehuda Benayahu[2]

[1]School of Mechanical Engineering, [2] School of Life Sciences
Tel-Aviv University, Tel Aviv 69978, Israel.

[*]Author for correspondence (zilman@eng.tau.ac.il)



## SUMMARY

Marine larvae are often considered as drifters that collide with larval collectors as passive particles. The trajectories of *Bugula neritina* larvae and of polystyrene beads were recorded in the velocity field of a vertical cylinder. The experiments illustrated that the trajectories of larvae and of beads may differ markedly. By considering a larva as a self-propelled mechanical microswimmer, a mathematical model of its motion in the two-dimensional velocity field of a long cylinder was formulated. Simulated larval trajectories were compared with experimental observations. We calculated the ratio $\eta$ of the probability of contact of a microswimmer with a cylinder to the probability of contact of a passive particle with the cylinder. We found that depending on the ratio $S$ of the swimming velocity of the microswimmer to the velocity of the ambient current, the probability of contact of a microswimmer with a collector may be orders of magnitude larger than the probability of contact of a passive particle with the cylinder: for S~0.01, $\eta$ ~1; for $S$~0.1, $\eta$~10; and for $S$~1, $\eta \sim 100$.

**KEYWORDS:** larvae; *Bugula neritina*; settlement; hydrodynamics; trajectories; self-propulsion; microswimmer; contact probability; cylinder.

**List of symbols**

Abbreviations**:** BL - boundary layer

Bold letters - **vectors**

$d_h$ - diameter of a helix

$d_p$ - equivalent diameter of a larva or particle

$D_c$ - diameter of a cylinder

$E_0$ - probability of contact of a particle with a collector

$E_S$ - probability of contact of a larva with a collector

**r** - radius vector of the centre of the particle

$R$ - radius of a cylinder

$\mathrm{Re}_c = \rho_f U_\infty D_c / \mu$ - the Reynolds number of a cylinder

$l_p = \rho_p d_p^2 U_\infty / 18\mu$ - the stopping distance a particle

$\mathrm{St}=l_p / D_c$ - the Stokes number

$t$ - time

$T$ - time period of a helix

**U** - flow velocity

$\mathbf{U}_\infty$ **-** flow velocity far from the collector

**V** - velocity of motion of a larva or particle

$\mathbf{V}_h$ - velocity of helical motion

$\mathbf{V}_S$ - swimming velocity of a larva

$V_t$ - sinking velocity of a larva

*oxyz* - helix-fixed Cartesian frame of reference

*OXYZ* - earth-fixed Cartesian frame of reference

$X_0, Y_0$ - initial coordinates of a larva or particle

$\boldsymbol{\gamma}$ - intrinsic angular velocity of a larva's helical motion

$\eta$ - normalised probability of contact of a larva, $E_S / E_0$

$\mu$ - water viscosity

$\rho_f$ - water density

$\rho_p$ - mean density of a larva or particle

$\phi$ - course (track) angle of a larva

$\phi_0$ - initial course angle of a larva

$\boldsymbol{\omega}$ - shear-induced angular velocity of a larva or particle

## INTRODUCTION

Contact of a marine invertebrate larva with an underwater surface necessarily precedes its attachment to the surface. However, not all larvae that contact a substrate attach to it. Therefore, the probability of contact represents the upper bound of the probability of settlement. The probability of contact is a quantitative characteristic of settlement, which is of great interest in marine biology, particularly if attachment follows the first contact event (Abelson and Denny, 1997; Mullineaux and Butman, 1991; Mullineaux and Garland, 1993).

It is common to distinguish between the settlement of larvae on substrates of infinite extent and settlement on bodies of finite size. Because of the wide variety of larval forms and collector types, it is also common to observe settlement of specific larvae (e.g., bryozoan *Bugula Neritina*) on relatively simple geometric forms, such as plates (Mullineaux and Butman, 1991; Mullineaux and Garland, 1993; Perkol-Finkel et al., 2008), cylinders (Harvey and Bourget, 1997; Rittschof et al., 2007) or inner sides of tubes (Crisp 1955; Qian et al., 1999, 2000). Here, we study the contact of *B. Neritina* larvae with a long vertical cylindrical collector.

Most natural larval collectors are covered by microbial films (e.g., Dexter 1979) or biofilms (e.g., Maki et al. 1989). The effect of microbial films and biofilms on bryozoan larval settlement has been observed both in the laboratory and under natural conditions (Brancato and Woollacott, 1982; Woollacott 1984; Woollacott et al. 1989; Maki et al., 1989; Callow and Fletcher, 1995). Generally, bryozoans are relatively indiscriminate settlers that may also settle on clean surfaces (Ryland, 1976; Dahms et al. 2004; Qian et al., 1999, 2000). We therefore used in our experiments a clean cylindrical collector that does not induce specific cues.

Chemical or physical cues play a central role in the behavioural biotic approach to larval settlement. In this approach a larva is attracted to a collector by cues and deliberately moves toward the collector. In an alternative mechanistic approach to larval settlement, a larva moves in the sea current as a drifter and collides with the collector as a

passive particle. The issue of passive vs. active contact has been intensively discussed in previous studies (Abelson et al., 1994; Butman, 1987; Butman et al., 1988; Harvey and Bourget, 1997; Harvey et al., 1995; Mullineaux and Butman, 1991; Mullineaux and Garland, 1993; Palmer et al., 2004).

However, the rich variety of models of larval contact with collectors can not be described solely in terms of the antonyms “active-passive”. Consider, for instance, a realistic scenario of a swimming larva that is not aware of a collector. A swimming larva is active by definition, but in the absence of biotic factors influencing its contact with a collector, the larva moves as a mechanical object, i.e., as a microswimmer (see, e.g., Kirbøe, 2008). Nonetheless, the hydrodynamics and dynamics of such a microswimmer can be rather complex and difficult to describe in detail. Therefore, mathematical modelling of the motion of a larva as a mechanical object is inevitably associated with considerable simplifications, which should however retain the most relevant problem parameters, such as the Reynolds number of the cylinder ($\mathrm{Re}_c$) and the Stokes number (St) of the particle-cylinder hydrodynamic system (Fuchs 1964; Friedlander 1977).

The Reynolds number $\mathrm{Re}_c = \rho_f U_\infty D_c / \mu$ represents the ratio of the inertial and viscous forces acting on a cylinder. It depends on the fluid density $\rho_f$, its viscosity $\mu$, the flow velocity far from the cylinder $U_\infty$ and the diameter of the cylinder $D_c$. The Stokes number represents the ratio of inertial and viscous forces acting on a particle that moves in the velocity field of the cylinder. The Stokes number depends on the parameters that determine $\mathrm{Re}_c$ and additionally on the parameters that determine a particle’s inertia, its characteristic size $d_p$ and its mean density $\rho_p$. A measure of the ratio of inertial and viscous forces acting on a particle is its stopping distance, $l_p = \rho_p d_p^2 U_\infty / 18\mu$, the distance at which a particle that starts its motion in a stagnant fluid with speed $U_\infty$ will be stopped by the drag force exerted on the particle by the fluid (Fuchs 1964). The dimensionless Stokes number is the ratio of the stopping distance of a particle to the characteristic size of the collector, $\mathrm{St} = l_p / D_c$ (Fuchs 1964). Whereas the shape of a collector and its Reynolds number determine the collector’s streamlines, the Stokes number characterises the degree of deviation of an inertial particle from the streamlines. The lower the Stokes number, the more a particle is “embedded” in the fluid. Low-inertia particles (St<~0.1)

follow streamlines rather closely and can be considered as inertialess particles, which follow streamlines exactly (Fuchs 1964; Friedlander 1977).

In contrast with passive particles, even an inertialess self-propelled microswimmer does not follow streamlines exactly. Zilman et al. (2008) theoretically studied the motion of a three-dimensional spherical microswimmer moving in a linear shear flow, in a channel flow, and in a Poiseuille tube flow and calculated the probability of contact of the microswimmer with the walls bounding the flows. Crowdy and Samson (2011) and Zöttl and Stark (2012) studied trajectories of a two-dimensional and three-dimensional microswimmer moving in linear and Poiseuille shear flows, and took into account not only the re-orientation effect reported in Zilman et al. (2008) but also the direct hydrodynamic interaction of the microswimmer with a plane substrate.

In this work, we consider a previously unstudied problem, the motion of a low-inertia microswimmer ($\mathrm{St} \ll 1$) in the velocity field of a large cylinder ($\mathrm{Re}_c = 10^2 - 10^5$). The aim of our study is to clarify how self-propulsion may influence the probability of contact of a microswimmer with a cylinder that does not induce biotic cues.

We observed the motion of *B. neritina* larvae in the velocity field of a cylinder and formulated a mathematical model of motion of a larva-microswimmer near the cylinder. We parameterised this mathematical model using experimental data, and calculated the probability of contact of larvae with a cylinder for a wide range of realistic problem parameters.

## MATERIALS AND METHODS

We collected sexually mature colonies of *B. neritina* from floating docks at the Tel-Aviv Marina in spring 2011-2012. Larvae of *B. neritina* were maintained in laboratory conditions following Qian et al. (1999) and Wendt (2000). The shape of *B. neritina* larva is close to a prolate spheroid, with a length-to-maximal-width ratio of approximately 1.1. Such a spheroid can be approximated by a sphere of volume equal to the volume of the larva of interest. The diameter of the equivalent sphere approximating *B. neritina* larva varies as $d_p = 200 - 350\ \mu$m (Kosman and Pernet, 2009; Wendt, 2000). The sinking velocity of an immobilised *B. neritina* larva is approximately $V_t = 1$ mm/s

(Koeugh and Black, 1996). Correspondingly, the ratio of the mean larva density $\rho_p$ to the water density $\rho_f$ is $\rho_p / \rho_f = 1.02 - 1.04$.

The motion of *B. neritina* larvae was observed in a transparent experimental flow tank (Figure 1). Larvae were gently pipetted into the tank, and their trajectories were recorded, both from above and from the side of the tank, using an Optronis GmbH (Germany) video system with two synchronised digital video cameras (500 fps and 1280x1024-pixel sensors) equipped with Nikkor (Japan) 60-mm/f2.8 or 100-mm/f2.8 macro lenses. The trajectories were digitised using the Matlab Image Processing Toolbox and an open source software package (http: //physics.georgetown.edu/matlab).

The flow velocity in the experimental flow tank was measured using the particle image velocimetry system from TSI Inc., which comprises a 120 mJ NewWave Solo dual-head Nd:YAG laser, a 4096 x 2048 pixel CCD camera with dynamic range 12 bits and a Nikkor 60-mm/f2.8 macro lens. Images were analysed using standard FFT-based cross-correlation algorithms and open-source software (http://www.openpiv.net) for verification purposes.

## EXPERIMENTAL RESULTS

### *Tank without a cylinder*

Typical trajectories of *B. neritina* larvae in still and moving water are shown in Figure 2. In still water, a *B. neritina* larva moves for distances of order of a few centimetres along a helix-like trajectory with an approximately straight axis but may also randomly change its direction of motion (Figure 2A). The helical portions of a larva's trajectory can be approximated by a regular helix with a straight axis *ox* that points in the direction of the vector of the larva's swimming velocity $\mathbf{V}_S$. A larva moves along a helical trajectory with linear velocity $\mathbf{V}_h$ and rotates with angular velocity $\boldsymbol{\gamma}$.

In a Cartesian coordinate system, *oxyz*, the coordinates $x_h, y_h, z_h$ of the centroid of a larva moving along a helical path vary with time *t* as $x_h = V_S t$, $y_h = 0.5 d_h \sin(\gamma t)$ and $z_h = 0.5 d_h \cos(\gamma t)$, where $d_h$ is the diameter of the helix. The projections of the total velocity of a point of a helix $\mathbf{V}_h(t)$ on the axes of the coordinate system *oxyz* can be

found as the time derivatives of the coordinates of the point of a helix, $dx_h/dt$, $dy_h/dt$, and $dz_h/dt$, thereby yielding the relation $V_S = \sqrt{V_h^2 - d_h^2\gamma^2/4}$.

The diameter of the helix $d_h$ and its temporary period $T$ can be estimated experimentally, as illustrated in Figure 2B. When a larva moves approximately horizontally, as in Figure 4B, which is discussed later, its swimming velocity $V_S$ can be calculated directly. When the trajectory of a larva does not belong to the plane of a lens, Wendt (2000) suggested estimating $V_h$ by filming the motion of the larva in a shallow depth of the field of the lens such that only a small portion of the trajectory is in focus. By calculating the velocity of a larva along this portion, one can estimate $V_h$.

According to our measurements, $V_S \approx 3-6$ mm/s, which is consistent with Wendt (2000). Once $V_S$, $d_h$ and $\gamma = 2\pi/T$ are known, the projections of the velocity $\mathbf{V}_h$ on the axes of the coordinate system *oxyz* can be found as time derivatives of the coordinates of the point of the helix $dx_h/dt$, $dy_h/dt$, and $dz_h/dt$.

When a larva moves in a unidirectional flow for which the velocity is much greater than the larva's swimming velocity, the helical trajectory of the larva stretches, straightens and becomes rather close to rectilinear streamlines (Figure 2C). Seemingly in such a case, a larva moves as a passive particle. However, the contact problem relates to larval motion in non-uniform velocity fields of a collector, where streamlines are curvilinear and the fluid velocity may be of the same order of magnitude as the swimming velocity of a larva. In the next sections, we compare the motion of a larva and of a passive particle in the velocity field of a cylinder.

## *Tank with a cylinder*

We studied trajectories of larvae, not the process of their attachment, because as stated in the introduction, attachment depends on the physiochemical properties of the surface of a collector. Figure 3A illustrates that the fluid velocity field in front of the cylinder is laminar and does not vary significantly between the horizontal planes $h = 15$ mm and $h = 27$ mm, where $h$ is measured from the bottom of the channel. Spherical polystyrene beads of $d_p = 430\,\mu$m diameter and of $\rho_p = 1.05\,g/\text{cm}^3$ density were pipetted into the flow and allowed to circulate in the tank before settling on the bottom.

Figure 3B shows typical trajectories of beads. A typical trajectory is characterised by smooth variation of its slope and smooth variation of its curvature; the latter changes the sign at a single inflection point of the trajectory. Using these criteria alone, one can infer that on many occasions, larvae also move along typical trajectories (Figure 3C). This similarity does not mean that a larva moves as a passive particle but only that the trajectory of a larva and that of a passive particle resemble one another as long as their slopes and curvatures vary in a similar manner.

However, in addition to the typical trajectories of larvae, we also observed a significant number of trajectories that we signify as atypical ($n$=23 in 560 tests) ( Figure 4). The atypical trajectories are characterised by an abrupt change in their slope at the points at which the distance between a larva and a cylinder's surface is minimal. No passive particle moves along such a trajectory. Thus, we suggest that atypical trajectories result from larval self-propulsion. Although the number of atypical trajectories is relatively small, they constitute the most salient qualitative manifestation of the influence of self-propulsion on larval trajectories in a non-uniform flow. Therefore, the atypical trajectories represent a considerable interest for our study. One of the aims of this work is to formulate a mathematical model of larval motion that is able to describe not only typical but also atypical trajectories.

## A MATHEMATICAL MODEL OF LARVAL CONTACT WITH A COLLECTOR

### *Larva-microswimmer*

A long vertical cylinder of diameter $D_c$ is placed in an unbounded two-dimensional rectilinear current. The vector of current velocity $\mathbf{U}_\infty$ is normal to the cylinder's axis and lies in the horizontal plane. The Reynolds number of the cylinder varies between $10^2$ and $10^5$, which implies that the flow at the front part of the cylinder is laminar (Schlichting, 1979). For the further analysis we use the following assumptions:

1) There is no hydrodynamic interaction between individual larvae;

2) A larva is small compared to a collector and to the characteristic linear scale of the spatial flow variations that are induced by the collector in a uniform current;

3) A small larva does not change the velocity field of the cylinder;

4) The sinking velocity of a larva is small compared to the fluid velocity and can be disregarded in the problem of larval contact with the vertical surface of a cylinder;

5) A larva's relative velocity with respect to shear flow is equal to the larva's relative velocity with respect to stagnant fluid;

6) The velocity field of the cylinder is two-dimensional; the vector of the fluid velocity **U** lies in the horizontal plane (Figure 5);

7) The vector of a larva's swimming velocity ($\mathbf{V}_S$) is perpendicular to the axis of the cylinder and lies in the plane of flow (Figure 5); the direction of $\mathbf{V}_S$ does not vary with respect to the rotating larva's body neither in stagnant nor in moving water;

8) In addition to an intrinsic self-induced rotation, a larva rotates as a small rigid sphere because of the shear-induced viscous torque;

Three primary mechanisms determine the collision of a passive particle: Brownian diffusion, inertial impaction, and direct interception (Fuchs, 1964; Kirbøe, 2008). If the diameter of the particle $d_p \gg 1\mu$m (which is always true for *B. neritina* larvae), Brownian diffusion does not influence the contact phenomenon under consideration (e.g., Kirbøe, 2008). The inertial impact is determined by the Stokes number of the problem. For the problem parameters adopted here, the Stokes number is much less than the threshold value 1/8, below which inertial impact of a spherical passive particle with a cylinder does not occur (Fuchs, 1964). Correspondingly, in our work, we consider only the mechanism of the direct interception. Within the framework of this mechanism a larva follows the streamlines of a collector exactly and collides with the collector because of the larva's finite size.

For the subsequent analysis, we adopt a mathematic model of larval helical motion suggested by Brokaw and generalised by Crenshaw (1989), in which the vectors of a larva's swimming velocity $\mathbf{V}_S$ and of its angular velocity $\boldsymbol{\gamma}$ are collinear and are directed along the same axis *ox* (Figure 5). Because the vector $\mathbf{V}_S$ lies in the horizontal plane, the vector $\boldsymbol{\gamma}$ is parallel to the horizontal plane. The vector of the angular velocity of the shear-induced rotation, $\boldsymbol{\omega} = 2^{-1}\mathrm{rot}\,\mathbf{U}$ (Lamb 1945), is perpendicular to vector of fluid velocity **U**. For a two-dimensional horizontal flow $\boldsymbol{\omega}$ is perpendicular to the horizontal plane and, thus, is perpendicular to $\boldsymbol{\gamma}$. The orthogonality of $\boldsymbol{\gamma}$ and $\boldsymbol{\omega}$ implies that shear-induced rotation of a larva does not change its intrinsic rotation about the axis *ox*.

In the earth-fixed frame of references, the direction of the larva's swimming velocity vector re-orients because of the larva's shear-induced rotation. The re-orientation effect of a larva's motion in the shear flow of a cylinder is illustrated in Figure 6. In the velocity field of a cylinder a larva moves along a curvilinear trajectory that can not be described as a helix with a straight axis, i.e., as a regular helix. In this respect, the shear flow influences the helical pattern of motion.

To calculate the fluid velocity field near the front part of a cylinder, we use the boundary layer (BL) theory and von-Karman-Pohlhausen's method, which is explained in detail in Schlichting (1979). In Figure 5, we provide a brief description of this method.

In the cylinder-fixed Cartesian coordinate system OXY (Figure 5), the linear velocity $\mathbf{V} = \mathbf{U} + \mathbf{V}_h$ of a massless swimmer can be represented as the time derivative of the radius vector of the centre of the swimmer $\mathbf{r}[X(t)\,Y(t)]$:

$$\frac{d\mathbf{r}}{dt} = \mathbf{V}(\mathbf{r})\,. \qquad (1)$$

The angular velocity of a larva $\omega$ about a vertical is equal to the time derivative of the track angle $\phi(t)$, the angle between the directions of the vectors $\mathbf{U}$ and $\mathbf{V}_S$ (Figure 5):

$$\frac{d\phi}{dt} = \omega(\mathbf{r})\,. \qquad (2)$$

Equations (1)-(2) determine the trajectory of a self-propelled larva microswimmer in the two-dimensional velocity field of a collector. For prescribed initial conditions of a swimmer $X(0) = X_0, Y(0) = Y_0$ and $\phi(0) = \phi_0$, we solve the differential equations (1)-(2) numerically using the 4$^{th}$-order Runge-Kutta method with an adaptive time step.

## THEORETICAL RESULTS VS. EXPERIMENTAL OBSERVATIONS

The degree of deviation of a microswimmer from the trajectory of a corresponding passive particle depends on the swimmer's velocity and on its initial conditions. Systematic numerical simulations show that depending on initial conditions, swimmers may move along typical or atypical trajectories. To calculate the trajectory of a microswimmer and compare it with an experimental trajectory of a larva, we must know the initial conditions of the larva's motion. Whereas the coordinates $(X_0, Y_0)$ can be measured with high accuracy, measurements of the course angle $\phi_0$ are difficult.

Therefore, we compare the computed trajectories of a microswimmer with the experimental trajectories of a larva for the same measurable coordinates $(X_0, Y_0)$ but for the track angle $\phi_0$ estimated iteratively as a problem parameter (Eykhoff, 1974).

Similarities between the calculated trajectories of a microswimmer and the observed trajectories of larvae (Figure 7) suggest that the main features of larval motion in the velocity field of a cylinder are faithfully captured by the mathematical model presented here. Although for each atypical trajectory, the match between theoretical and experimental data was obtained for a particular initial angle $\phi_0$ and a particular coordinate $Y_0$, the general character of atypical trajectories is determined by the local fluid mechanics in the closest vicinity of a collector, i.e., in its BL.

A trajectory of a larva defines a contact event. Thus using the same mathematical model, we can calculate the trajectory of a larva and the probability of its contact with a cylinder.

## THE PROBABILITY OF CONTACT OF A MICROSWIMMER WITH A COLLECTOR

In the theory of aerosols (Fuchs, 1964), one of the methods of evaluating the probability of contact (collision) of passive particles with a collector ($E_0$), is based on the analysis of their trajectories. The trajectory analysis is applied here to calculate the probability of contact of a microswimmer with a collector ($E_S$). The mathematical details of the trajectory analysis are provided in Figure 8. Satisfactory agreement between the theoretical and available experimental data of contact probability for passive particles, illustrated in Figure 9, suggests that the mathematical model we used to calculate the contact probability of passive particles can also be used to calculate the contact probability of microswimmers.

Now, we return to the central question of our work: "How does a larva's self-propulsion influence the probability of its contact with a collector if the larva is not aware of the collector?" We characterise this influence as the ratio $\eta = E_S / E_0$, which is plotted in Figure 10 for a wide range of realistic problem parameters adopted here.

## DISCUSSION

We observed trajectories of larvae *B. neritina* and of passive particles that mimic larvae in the velocity field of a vertical cylinder (Figure 3 - Figure **4**). We revealed a considerable number of larval trajectories that differed markedly from the trajectories of passive particles ( Figure **4**). We attributed such trajectories to larval self-propulsions. To explain our experimental observations, we formulated a mathematical model of a larva's motion in the two-dimensional laminar velocity field of a long cylinder ($10^2 < \mathrm{Re}_c < 10^5$). The validity of our mathematical model is confirmed by satisfactory qualitative agreement between the experimental trajectories of larvae and the simulated trajectories of a microswimmer (Figure 7) and by satisfactory quantitative agreement between simulated and measured probabilities of contact with a cylinder of passive particles (Figure 9).

Using trajectory analysis and Monte Carlo simulations, we calculated the probability of contact of a microswimmer with the front part of a cylinder. Mathematical modelling revealed a considerable increase in the probability of contact of the microswimmer with a cylinder compared to the probability of contact with the same cylinder of the same microswimmer but with zero swimming velocity, $\eta = E_S / E_0$ (Figure 11). Regarding orders of magnitude, this increase can be estimated as follows: for $V_S / U_\infty \sim 0.01$, $\eta \sim 1$; for $V_S / U_\infty \sim 0.1$, $\eta \sim 10$; and for $V_S / U_\infty \sim 1$, $\eta \sim 10^2$. For instance, because of self-propulsion, larvae of *B. Neritina* with the swimming velocity ~5 mm/s may increase their probability of contact with a cylinder 10-fold in a sea current of ~5 cm/s and 100-fold in a sea current ~2.5 cm/s. Although sea currents of 2.5-5 cm/s are rare, our theoretical prediction is consistent with the observations of Qian et al. (1999, 2000): in tubes with laminar flow, larvae of *B. Neritina* preferred to settle in low-speed currents *U*~2.5 cm/s; whereas for *U*>~8 cm/s, the probability of settlement drastically decreased. It should also be noted that some biofouling marine larvae swim much faster than larvae of *B. Neritina* (Table 1). For those larvae, the ratio $V_S / U_\infty > 0.1$, which provides a ~10-100-fold increase in the probability of contact, may correspond to frequent currents of the order of tens of cm/s. (Table 1). In contrast, within the framework of a mechanistic approach and according to the results of our mathematical

modelling, larvae with $V_S <\sim 2$ mm/s that move in sea current $U_\infty >\sim 5$ cm/s make contact with a collector as passive particles.

We formulated the problem of larval contact with a collector for a spherical microswimmer. However, a small sphere and a small spheroid of moderate slenderness ~1.5-2.0 (such as the larvae listed in Table 1) move in a linear shear flow along similar trajectories (Zöttl and Stark, 2012). Given that a BL without separation can be approximated by a linear shear flow for qualitative estimates (Schlichting, 1979), it is not unlikely that a spheroidal swimmer may move in the two-dimensional BL approximately as a spherical swimmer.

We formulated the problem of contact of a microswimmer with a cylinder for laminar flows $\mathrm{Re}_c \gg 1$. Experimental data regarding settlement (not contact specifically) of marine larvae on a cylinder in a natural turbulent environment were reported by Rittschof et al. (2007). We did not find experimental or theoretical works in which the probability of contact of swimmers with a cylinder in turbulent flows was measured or calculated for $\mathrm{St} \ll 1$ and $\mathrm{Re}_c \gg 1$. For such flow parameters the available and rather limited experimental data pertain only to contact of passive particles with a cylinder. Asset et al. (1970) and Stuempfle (1973) reported that for Stokes and Reynolds numbers such as those studied here, incoming upstream turbulence with an intensity of less than 7-8% practically does not affect the probability of contact of passive particles with a cylinder. In strong turbulence, the swimming speed of a larva may be small compared with the turbulent fluctuations of the fluid velocity. In such cases, a larva's self-propulsion may have little effect on its trajectory except in the vicinity of the collector, where the fluid velocity and its turbulent fluctuations are low (Schlichting 1979).

The hydrodynamic model of contact of a microswimmer with a cylinder proposed here may be relevant for self-propelled larvae and aquatic larval collectors, such as kelp stems, sea grasses, small artificial reefs, pillars, columns, and other engineering structures, that are located in a relatively slow sea current of low-to-moderate turbulent intensity (Abelson et al., 1994). Mathematical modelling of the motion of a larva in the velocity field of a collector located in a fully turbulent environment is beyond the scope of our present work.

In conclusion, the results of our investigation, which are presented in Figure 10, suggest that for the problem parameters presented here, self-propulsion may greatly

increase a larva's odds of making contact with the collector even if the larva does not detect the collector remotely.

**Acknowledgments**

This work was supported by the Israeli Science Foundation Research Grant 1404/09. The authors are grateful to R. Strathman and M. Hadfield for constructive discussions. L. Kagan, J. Pechenic and L. Shemer read the manuscript and made many valuable comments. G. Gulitsky is acknowledged for the assistance in the design of the experimental flow tank and N. Paz for editorial works.



**References**

**Abelson, A., and Denny, M.** (1997). Settlement of marine organisms in flow. *Annual Review of Ecology and Systematics* 28, 317-339.

**Abelson, A., Weihs, D., and Loya, Y.** (1994). Hydrodynamic Impediments to Settlement of Marine Propagules, and Adhesive-Filament Solutions. *Limnology and Oceanography* 39, 164-169.

**Asset, G., Kimball, D., and Hoff, M.** (1970). Small-Particle Collection Efficiency of Vertical Cylinders in Flows of Low-Intensity Turbulence. *American Industrial Hygiene Association Journal* 31, 331-334.

**Brancato, M.S., Woollacott, R.M. (**1982). Effect of microbial films on settlement of bryozoan larvae (Bugula simplex, B. stolonifera and B. turrita). Mar. Biol. 71, 51– 56.

**Bryan, J.P., Rittschof, D., Qian, P.-Y**. (1997). Settlement inhibition of bryozoan larvae by bacterial films and aqueous leachates. *Bull. Mar. Sci.* 61, 849– 857.

**Butman, C.A.** (1987). Larval Settlement of Soft-Sediment Invertebrates - the Spatial Scales of Pattern Explained by Active Habitat Selection and the Emerging Role of Hydrodynamical Processes. *Oceanography and Marine Biology* 25, 113-165.

**Butman, C.A., Grassle, J.P., and Webb, C.M.** (1988). Substrate choices made by marine larvae settling in still water and in a flume flow. *Nature* 333, 771-773.

**Callow, E.M., and Fletcher, R.L.** (1995). The influence of low surface energy materials on bioadhesion-a review. *International Biodeterioration & Biodegradation* 34, 333-348.

**Crisp, D.J.** (1955). The behavior of barnacle cyprids in relation to water movement over a surface. *The Journal of Experimental Biology* 32, 569-590.

**Dahms, H-U., Dobretsov, S. and Qian, P-Y.** (2004). The effect of bacterial and diatom biofilms on the settlement of the bryozoan Bugula neritina, Journal of Experimental Marine Biology and Ecology 313, 191– 209.

**Dexter, S.** (1979). Influence of substratum critical surface tension on bacterial adhesion—*in situ* studies *J. Colloid Interface Sci.*70, 346–54

**Eykhoff, P.** (1974). System Identification Parameter and State Estimation. John Wiley & Sons, New York. 555 pp.

**Friedlander, S.K.** (1977). Smoke, dust, and haze : fundamentals of aerosol behavior. J. Wiley, New York. 317 pp.

**Fuchs, N.A.** (1964). The mechanics of aerosols. Pergamon Press, Oxford. 408 pp.

**Harvey, M., and Bourget, E.** (1997). Recruitment of marine invertebrates onto arborescent epibenthic structures: active and passive processes acting at different spatial scales. *Marine Ecology-Progress Series* 153, 203-215.

**Harvey, M., Bourget, E., and Ingram, R.G.** (1995). Experimental-Evidence of Passive Accumulation of Marine Bivalve Larvae on Filamentous Epibenthic Structures. *Limnology and Oceanography* 40, 94-104.

**Kirbøe, T.** (2008). A mechanistic approach to plankton ecology. Princeton University Press, Princeton. 209 p pp.

**Koeugh, H.J., and Black, K.P.** (1996). Predicting of scale of marine impact: understanding planktonic link between populations. In Detecting Ecological Impact. R. Schmitt, and C.W. Osenberg, editors. Academic Press, 199-234.

**Kosman, E.T., and Pernet, B.** (2009). Diel Variation in the Sizes of Larvae of Bugula neritina in Field Populations. *Biological Bulletin* 216, 85-93.

**Lamb, H.** (1945). Hydrodynamics. Dover, New York. 533 p pp.

**Maki, J.S., Rittschof, D., Schmidt, A.R., Snyder, A.G. and Mitchell, R.** (1989). Factors controlling attachment of bryozoan larvae: a comparison of bacterial films and unfilmed surfaces. The Biological Bulletin 177, 295–302.

**Mullineaux, L.S., and Butman, C.A.** (1991). Initial Contact, Exploration and Attachment of Barnacle (Balanus-Amphitrite) Cyprids Settling in Flow. *Marine Biology* 110, 93-103.

**Mullineaux, L.S., and Garland, E.D.** (1993). Larval Recruitment in Response to Manipulated Field Flows. *Marine Biology* 116, 667-683.

**Palmer, M.R., Nepf, H.M., and Pettersson, T.J.R.** (2004). Observations of particle capture on a cylindrical collector: Implications for particle accumulation and removal in aquatic systems. *Limnology and Oceanography* 49, 76-85.

**Perkol-Finkel, S., Zilman, G., Sella, I., Miloh, T., and Benayahu, Y.** (2008). Floating and fixed artificial habitats: Spatial and temporal patterns of benthic communities in a coral reef environment. *Estuarine Coastal and Shelf Science* 77, 491-500.

**Qian, P-Y., Rittschof, D., Sreedhar, B., and Chia, F.S.** (1999). Macrofouling in unidirectional flow: miniature pipes as experimental models for studying the effects of hydrodynamics on invertebrate larval settlement. *Marine Ecology-Progress Series* 191, 141-151.

**Qian, P-Y., Rittschof, D., and Sreedhar, B.** (2000). Macrofouling in unidirectional flow: miniature pipes as experimental models for studying the interaction of flow and surface characteristics on the attachment of barnacle, bryozoan and polychaete larvae. *Marine Ecology-Progress Series* 207, 109-121.

**Rittschof, D., Sin, T.M., Teo, S.L.M., and Coutinho, R.** (2007). Fouling in natural flows: Cylinders and panels as collectors of particles and barnacle larvae. *Journal of Experimental Marine Biology and Ecology* 348, 85-96.

**Ryland J.S.** (1976). Physiology and ecology of marine bryozoans. *Advances in Marine Biology* 14, 285-443.

**Schlichting, H.** (1979). Boundary layer theory. McGraw-Hill, New York. 535 pp.

**Stuempfle, A.K.** (1973). Impaction efficiency of cylindrical collectors in laminar and turbulent fluid flow. In Part III.Experimental. Edgewood arsenal technical report AD909457. Department of the Army, Headquarters, Edgewwod Arsenal, Maryland. 44

**Walker, G. and Lester, R.J.G.** (2000). The cyprids larvae of parasitic barnacle Heterosaccus lutanus (Crustacea, Cirripedia, Rhizocephala): some laboratory observations. Journal of Experimental Marine Biology and Ecology 254, 249-257.

**Walker, G**. (2004). Swimming speeds of the larval stages of the parazitic barnacle, Heterosaccus lunatus (Crustacea: Ciripedia: Rhizocephala), *Journal of Marine Biological Association UK* 84, 737-742.

**Wendt, D.E.** (2000). Energetics of larval swimming and metamorphosis in four species of *Bugula* (Bryozoa). *Biological Bulletin* 198, 346-356.

**Woollacott, R.M. (**1984). Environmental factors in bryozoan settlement. In: Costlow, J.D., Tipper, R.C. (Eds.),Marine Biodeterioration, an Interdisciplinary Study. Naval Institute Press, Annapolis, pp. 149– 154.

**Woollacott, R.M., Pechenik, J.A., Imbalzano, K.M. (**1989). Effects of duration of larval swimming period in early colony development in Bugula stolonifera (Bryozoa: Cheilostomata). Mar. Biol. 102, 57– 63.

**Zilman, G., Novak, J., and Benayahu, Y.** (2008). How do larvae attach to a solid in a laminar flow? *Marine Biology* 154, 1-26.

**Zilman, G., Novak, J., Liberzon, A., Perkol-Finkel, S., and Benayahu, Y.** (2011). Role of self-propulsion of marine larvae on their probaility of contact with a protruding collector located in a sea current. *arXiv preprint arXiv: 1108.1558*

**Zöttl, A., and Stark, H.** (2012). Nonlinear Dynamics of a Microswimmer in Poiseuille Flow. *Physical Review Letters* 108, 218104(218104).

Table 1. Fast larvae of marine invertebrates settling on protruding collectors.

| Taxon | Swimming speed<br><br>cm/s | Source | Current velocity corresponding to $\eta = 10$<br>cm/s | Current velocity corresponding to $\eta = 100$<br>cm/s |
|---|---|---|---|---|
| *Semibalanus balanoides* | 4.8.-5.4 | Crisp (1955), Walker (2004) | 68.5-77.1 | 24-27 |
| *Balanus crenatus* | 3.9 | Crisp (1955) | 55.7 | 19.5 |
| *Heterosaccus lunatus* | 1.8-2.8 | Walker & Lester (2004) | 25.7-40.0 | 9.0-14.0 |
| *Sacculina carcini* | 1.3-1.8 | Walker & Lester (2004) | 18.6-25.7 | 6.5-8.0 |
| *Hydroides elegans* | 1.5 | Qian et al. (1999) | 21.4 | 7.5 |

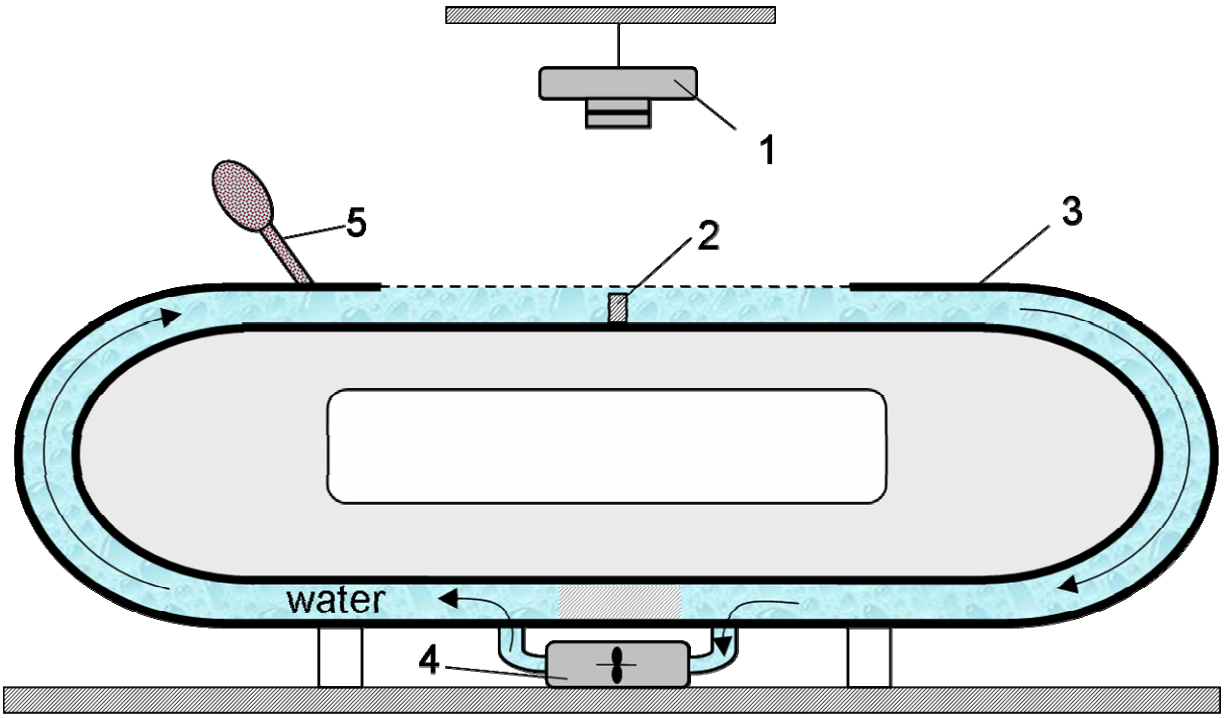


Figure 1**.** The experimental setup (not to scale). 1 - top-view video camera; 2 - cylinder; 3 - flow tank; 4 - water pump. Transparent Plexiglas plates form a channel of length $\approx 1.7$ m, width = 20 mm and height = 40 mm. A Plexiglas cylinder of diameter $D_c = 10$ mm and height = 30 mm can be mounted in the middle of the channel. A solution of artificial seawater was circulated in the channel using a pump driven by an electric motor. The flow velocities were controlled in the range 1-6 cm/s.

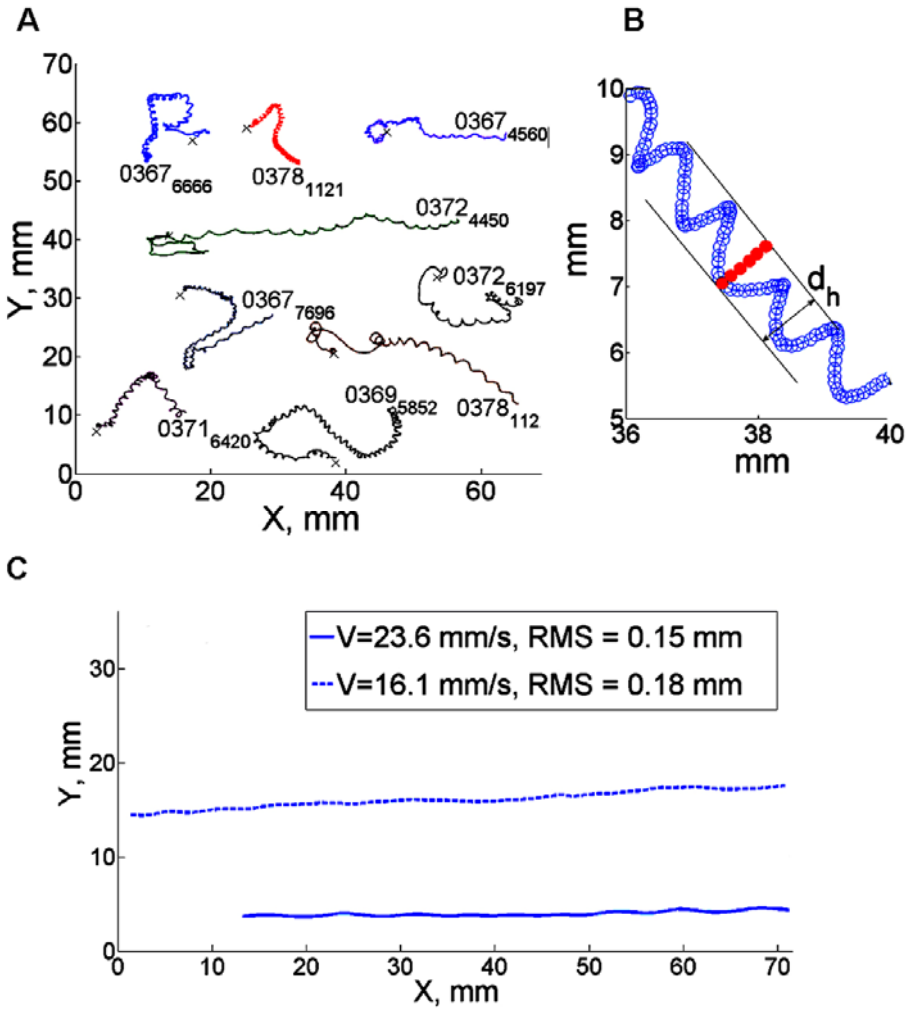


Figure 2. Trajectories of larvae in a flume without a cylinder.
(A) Still water. × denotes the beginning of the trajectory. Phototactile larvae biased their movements (from left to right in the figure) towards the illuminated side of the tank.
(B) Enlarged part of trajectory $0369_{0582}$. Open circles denote the consequent position of a larva at a resolution of 1/24 s. Full red circles depict the estimated transverse displacement of larvae in the direction perpendicular to the direction of swimming measured in larval diameters. The radius of the diameter of a helix can be estimated as approximately six larval diameters, the temporal period of the helix $T$ can be estimated as approximately 1 s. The angular frequency of helical motion can be estimated as approximately 6.3 rad/$s^{-1}$.
(C) Motion of larvae in running water. The root mean square deviation of the larva from a straight path is of the same order of magnitude as the deviation of a larva from the axis of a helix.

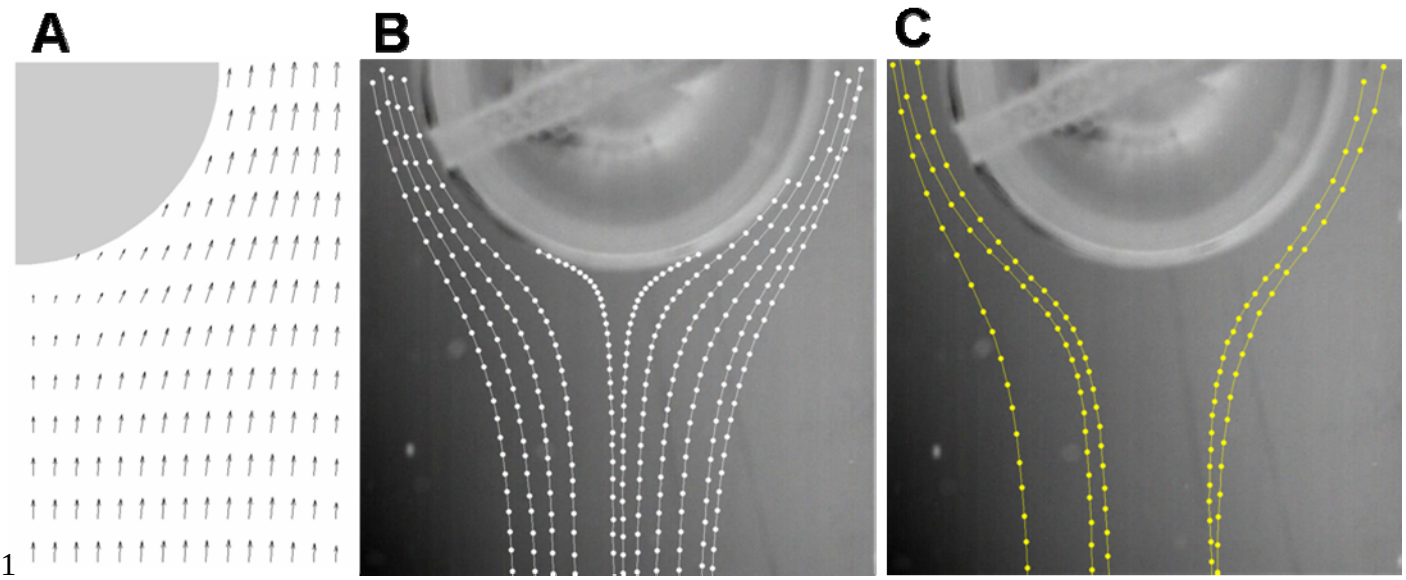


Figure 3. Fluid velocity in a tank with a cylinder and trajectories of beads and larvae ($D_c = 0.01$ m, $U_\infty = 0.03$ m/s, $\mathrm{Re}_c = 300$).
(A) Velocity field at the distance $h_1 = 27$ mm measured from the bottom of the flume. The velocity fields in the planes $h_2 = 22$ mm and $h_3 = 15$ mm are similar to those presented here.
(B) Trajectories of spherical beads approaching the cylinder.
(C) Trajectories of *B. Neritina* in the velocity field of a cylinder, which are similar to the trajectories of beads.

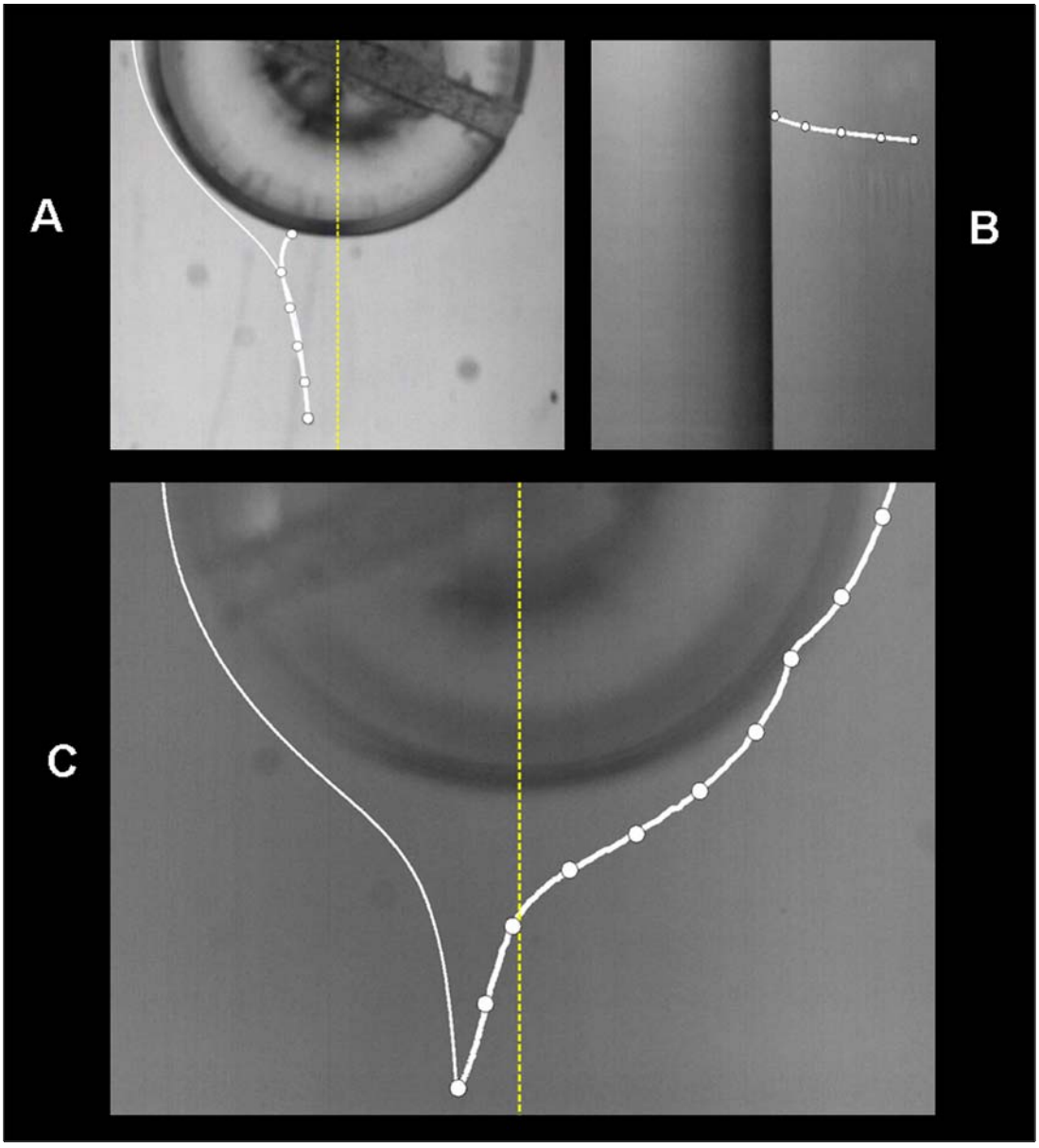


Figure 4. Motion of a passive particle and a larva near a cylinder for the problem parameters given in Figure 3. The lines with circular symbols indicate larvae. The lines without symbols indicate simulated trajectories of passive particles.
(A-B) Trajectory of a larva with contact and attachment. A - view from above; B - side view. After contact, the larva remains on the cylinder.
(C) A larva approaches the cylinder closely but without attachment; the view is from above.
A passive particle and a larva that start their motion at the same point move along different trajectories.

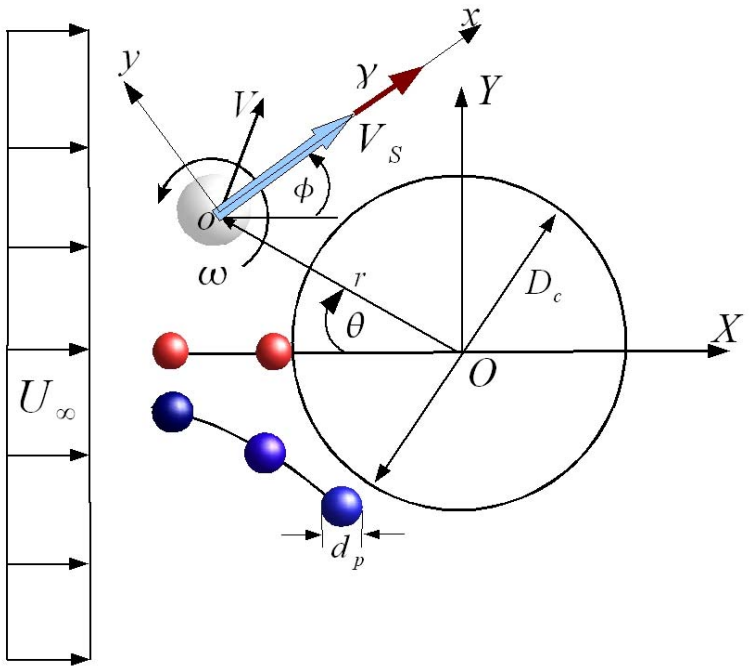


Figure 5. Velocity field induced by the cylinder. The origin $O$ of the cylinder-fixed coordinate system $OXYZ$ coincides with the centre of the cylinder. The axis $OX$ is collinear with the velocity vector $\mathbf{U}_\infty$. The coordinates of the centre of a microswimmer are defined by the radius-vector $\mathbf{r}$. The orthogonal coordinate system *oxyz* translates with the velocity of the centre of the microswimmer V and rotates with the shear-induced angular velocity $\omega$. The vector of the swimming velocity $\mathbf{V}_S$ of the microswimmer is directed along the axis $ox$ and constitutes with the axis *OX* the course angle $\phi$. The vector angular velocity of the microswimmer $\boldsymbol{\gamma}$ is collinear with $\mathbf{V}_S$. Rotation of a spherical microswimmer about the axis $ox$ does not influence the trajectory of the microswimmer in the plane $OXY$. The auxiliary polar angle $\theta = \arctan(Y/X)$ is used here for calculating the velocity field around the cylinder. Outside the boundary, the fluid can be considered as inviscid and its motion as irrotational. Thus, the velocity field of a cylinder can be calculated as for a potential flow (Lamb, 1945). In the boundary layer, the fluid velocity component parallel to the contour of the cylinder is defined as $u_\theta = U(\theta)[F(\eta) + \Lambda(\theta)G(\eta)]$, where $U(\theta)$ is the fluid velocity at the contour of the boundary layer of thickness $\delta(\theta)$, $F(\eta)$ and $G(\eta)$ are given polynomials of a non-dimensional coordinate $\eta = (r - D_c/2)/\delta$, and the tabulated values of $\delta(\theta)$ and $\Lambda(\theta)$ are provided in (Schlichting, 1979). Once $u_\theta$ is known, the fluid velocity component $v_r$ in the direction normal to the contour of the cylinder can then be obtained using the equation of mass conservation. Projecting $(u_\theta, v_r)$ onto the axes of the coordinate system OXY, we obtain $\mathbf{U}$ and $\boldsymbol{\omega} = 2^{-1}\mathrm{rot}\,\mathbf{U}$, which are involved in (1)-(2).

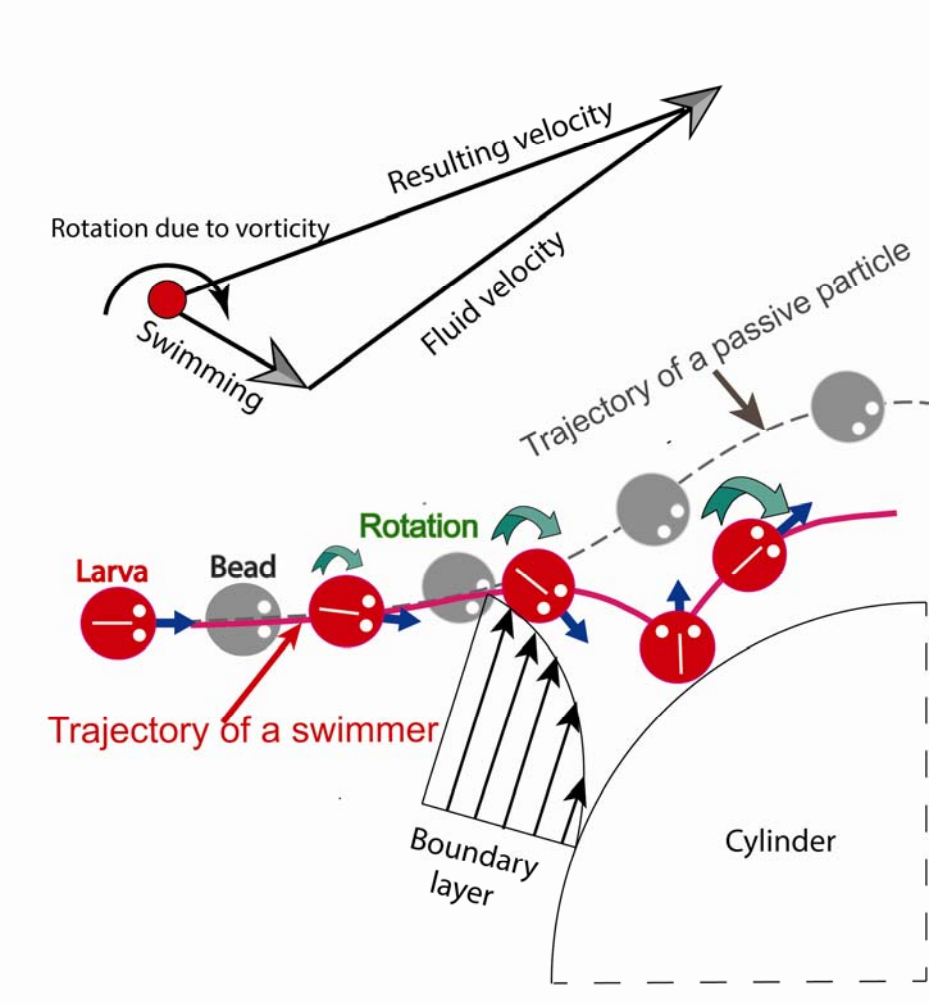


Figure 6. Schematic trajectories of motion of a larva. Motion of a passive particle (grey symbols) and a microswimmer (red symbols) in the boundary layer of a collector. The linear velocity of a microswimmer is the geometrical sum of the flow velocity and the velocity of the swimmer. Because of translation, the microswimmer does not move along the trajectory of a passive particle. Additionally, both the microswimmer and the passive particle rotate due to boundary layer vorticity. The vector of the angular velocity of the shear-induced rotation is normal to the plane of the paper. For a spherical particle, the rotation does not influence its trajectory. A rotating microswimmer re-orientates and further deviates from the trajectory of a passive particle. A small passive particle in the velocity field of a large collector moves along a streamline, which does not cross the cylinder. Deviation of a swimmer from the trajectory of a passive particle may result in its contact with the cylinder with much higher probability than the probability of contact with the cylinder of a passive particle.

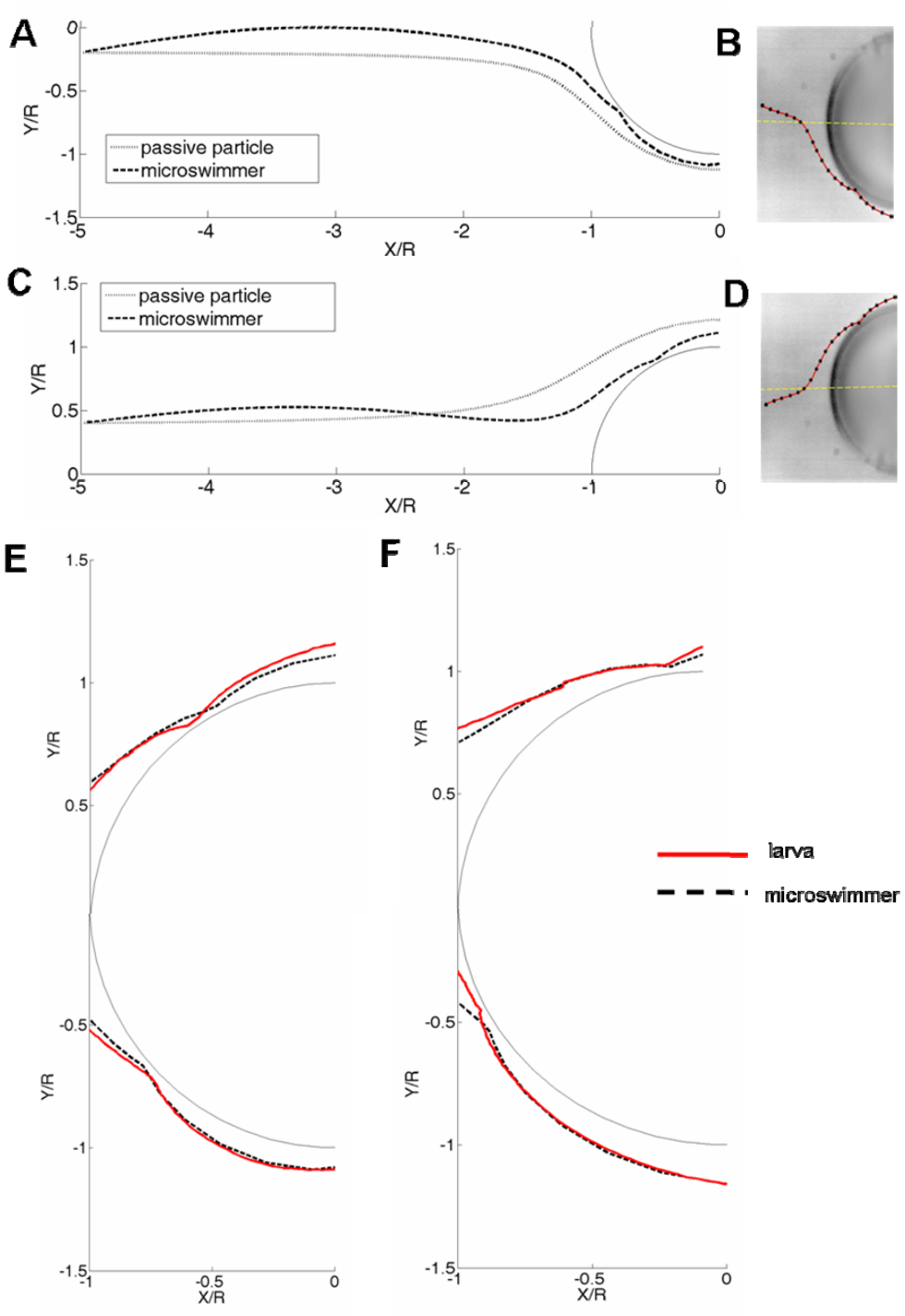


Figure 7. Trajectories of a passive particle, microswimmer and a larva near a cylindrical collector ($D_c = 0.01$ m, $d_p = 250$ $\mu$m, $V_S = 0.005$ m/s, and $\mathrm{Re}_c = 300$). The coordinates are normalised by the radius of the cylinder $R$ ($X_0 / R = -5.0$).
(A-B) $Y_0 / R = -0.2$, $\phi_0 = 12.2^\circ$; (C-D) $Y_0 / R = 0.4$, $\phi_0 = -10.2^\circ$.
(E- F) Enlarged parts of larval trajectories in the closest vicinity of the cylinder.

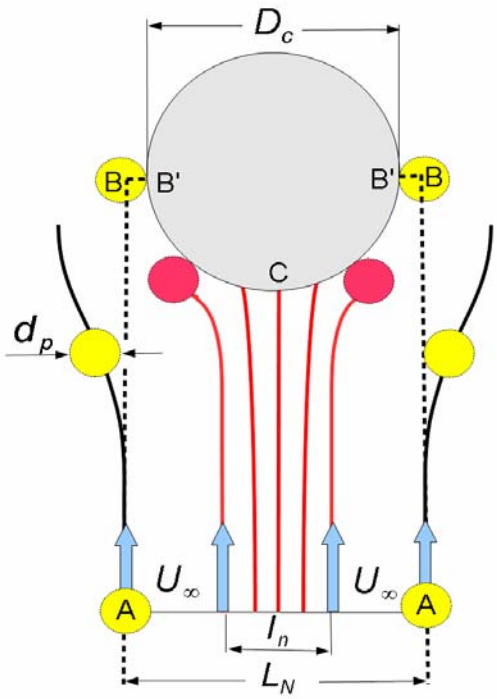


Figure 8. Geometrical definition of the probability of contact (not to scale). The motion of particles (yellow circles) is tracked in the control volume ABB'CB'BA, which is fully penetrable except at the contour of the cylinder. Contact is assumed to occur if the distance from the centre of a particle to the cylinder is equal to the radius of the particle. Red lines and red circles represent the limiting (grazing) trajectories that for passive particles can be calculated iteratively, thereby yielding an estimate of the probability of contact $E_0 = l_n / L_n$. The method of grazing trajectories cannot be applied for swimmers because they start their motion with random angles of swimming. Instead, Monte Carlo simulations can be used as an alternative method of calculating of the probability of contact. It is possible to calculate the number of particles that contact the collector by tracking the trajectories of *N* particles that start their motion far from a cylinder with random uniformly distributed initial coordinates $-R < Y_0 < R$ $(R = D_c / 2)$. The ratio of $n$ particles that contact the cylinder to the total number of the particles *N* determines the probability of contact, $E_0 = n / N$. To compare the probability of contact of passive particles $E_0$ with that of swimmers $E_S$, we must account for the randomness not only of the initial coordinate of the swimmer $Y_0$ but also of the initial track angle $\phi_0$. Assume now that $N_S$ microswimmers start their motion with random uniformly distributed coordinates $-R < Y_0 < R$ and random uniformly distributed angles $0 < \phi_0 < 2\pi$. Then, the ratio of $n_S$ microswimmers that collide with the collector to the total number of the microswimmers $N_S$ yields an estimate of the probability of contact of microswimmers, $E_S = n_S / N_S$ (Sobol 1994). To obtain robust results, we repeated Monte Carlo simulations by doubling the number of testing points until the error of the estimate of the probability of contact was less than 5%. To obtain this degree of accuracy, we used $N_s \propto 10^5$ test microswimmers.

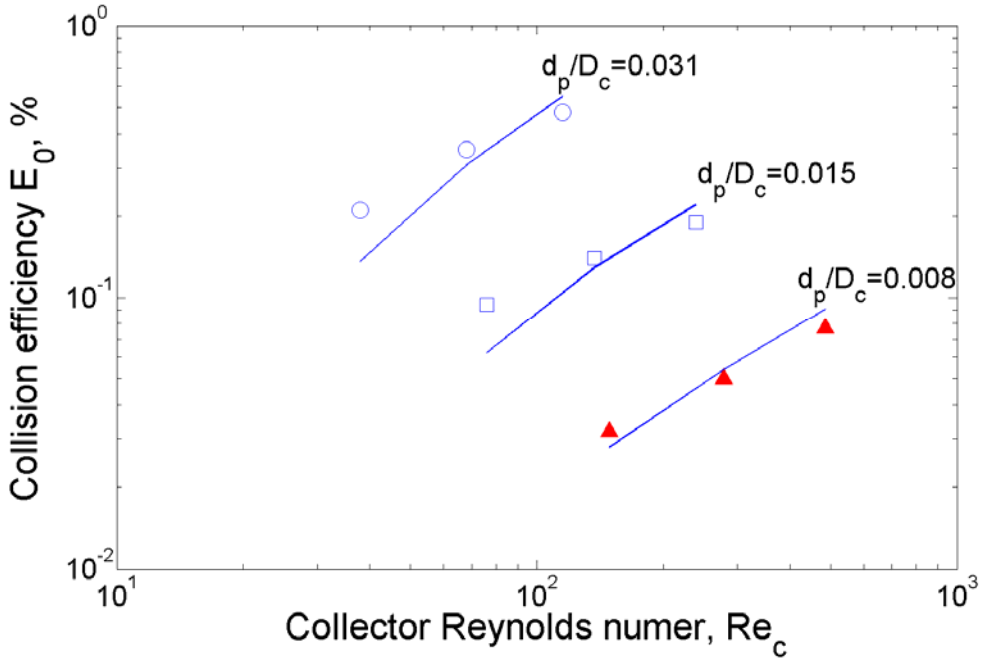


Figure 9. Probability of contact of passive particles ($d_p = 194\ \mu$m). Solid lines – our numerical simulations. Symbols pertain to experimental values obtained by Palmer et al. (2004), who observed capture of spherical particles of diameter $d_p \approx 194\mu$m on a long vertical cylindrical of diameter of 0.63-2.54 cm in laminar flow ($d_p / D_c = 0.083$-$0.31,\ \mathrm{Re}_c = 68 - 486$). The conditions of the Palmer et al. (2004) experiment match the assumption of our mathematical model. A discrepancy between the theoretical and experimental results can be observed in the range of Reynolds numbers less than 100, where the theory of the boundary layer is not expected to be accurate (Friedlander, 1977).

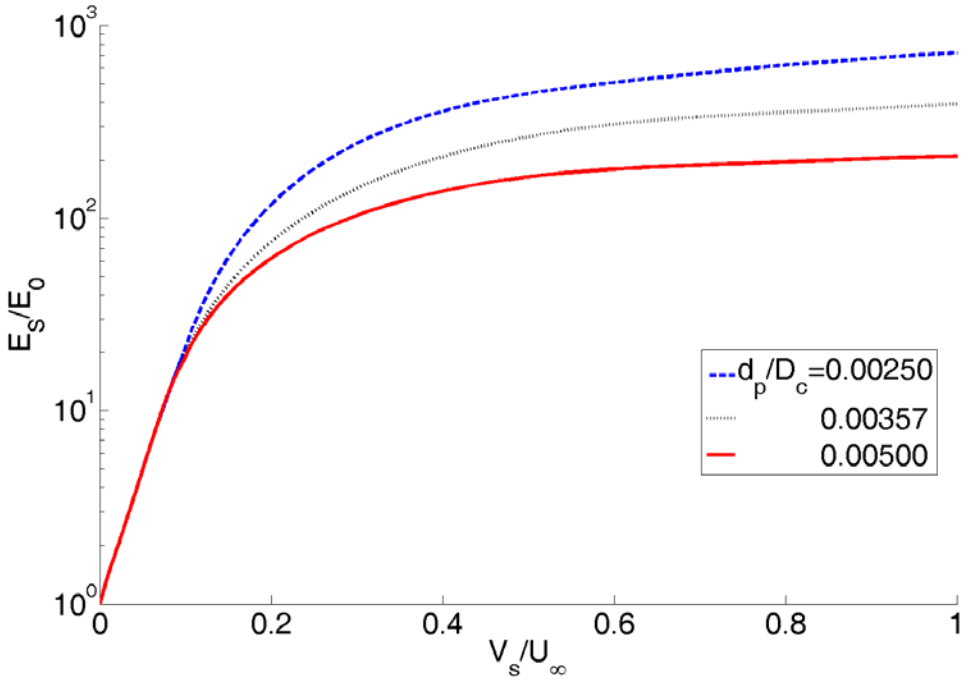


Figure 10. Simulated probability of contact of self-propelled particles normalised by the probability of contact of passive particles ($V_S = 0.005$ m/s, $d_p = 250\ \mu$m, $\mathrm{Re}_c = 2\times10^2 - 10^4$). In this figure the numerical simulations are performed for parameters of a regular helix $d_h = 6d_p$, $\gamma = 6.3$ rad/s. Systematic numerical simulations show that for $d_p = 0$ the presented here results remain approximately the same. That implies that for the presented here problem parameters the helical motion, including its irregularities, does not affect significantly the probability of contact.